Biochemical and Biophysical Research Communications 438 (2013) 318–323

Contents lists available at SciVerse ScienceDirect

Biochemical and Biophysical Research Communications

journal homepage: www.elsevier.com/locate/ybbrc

Kamolonol suppresses angiotensin II-induced stress fiber formation and cellular hypertrophy through inhibition of Rho-associated kinase 2 activity

Mun Sun Kim [a,b,1], Kwang-Seok Oh [a,1], Jeong Hyun Lee [a], Shi Yong Ryu [c], Jihye Mun [a], Byung Ho Lee [a,b,*]

[a] Research Center for Drug Discovery Technology, Korea Research Institute of Chemical Technology, Daejeon 305-343, Republic of Korea
[b] Graduate School of New Drug Discovery and Development, Chungnam National University, Daejeon 305-764, Republic of Korea
[c] Research Center for Medicinal Chemistry, Korea Research Institute of Chemical Technology, Daejeon 305-343, Republic of Korea

ARTICLE INFO

Article history:
Received 18 June 2013
Available online 24 July 2013

Keywords:
Kamolonol
Rho-associated kinase
Angiotensin II
Actin stress fiber
Cellular hypertrophy

ABSTRACT

Kamolonol (7-[[(1*R*,2*R*,4*R*,4a*S*,5*R*,8a*S*)-4-hydroxy-1,2,4a,5-tetramethyl-6-oxo-3,4,5,7,8,8a-hexahydro-2H-naphthalen-1-yl]methoxy]chromen-2-one) is a sesquiterpene coumarin and an active component of gum extracts from *Ferula assafoetida*. The aim of this study was to investigate the anti-fibrotic and anti-cellular hypertrophic effects of kamolonol, and further to explore its possible mechanism. Kamolonol (3–30 μM) significantly inhibited stress fiber formation induced by angiotensin II (Ang II) in rat heart-derived H9c2 cells. Furthermore, kamolonol (3–30 μM) showed a potent inhibitory effect on Ang II-induced cellular hypertrophy in H9c2 cells. Next, a Rho-associated kinase (ROCK) activity was measured because actin stress fiber formation and/or cellular hypertrophy are usually induced by the activation of ROCK. Rho-associated kinase 2 (ROCK2) studies using a time-resolved fluorescence resonance energy transfer (TR-FRET) showed that kamolonol possesses a potent ROCK2 inhibitory activity with IC_{50} values of 2.27 μM, and has an ATP-competitive inhibitory mode. In validation study, pretreatment of kamolonol (3–30 μM) for 2 h decreased the Ang II-induced phosphorylation of myosin phosphatase 1 (MYPT1) and myosin light chain 2 (MLC2). Taken together, these results indicate that kamolonol suppresses Ang II-induced stress fiber formation and cellular hypertrophy, and propose that one mechanism underlying these anti-fibrotic and anti-cellular hypertrophic effects involves inhibition of the ROCK-MLC pathway.

1. Introduction

Stress fibers are commonly thought as cytoskeletal structures found along the basal plasma membrane. These structures are actin myosin-based contractile systems and seen as bundles of actin filaments. Some of these bundles are less suited for cell motility and more suited to static contraction [1]. However, inappropriate regulation of stress fiber formation is directly involved in numerous pathological situations, including cardiovascular disease and cancer [2,3]. In fact, stress fibers are commonly observed in nearly all major cardiovascular diseases including hypertension, cardiomyopathy and heart failure, as well as cardiac remodeling after myocardial infarction [4]. As such, the inhibition of stress fiber formation has been considered to provide a pharmacological strategy for preventing and treating cardiovascular diseases. Although the exact mechanism is still eluted, Rho-associated kinase (ROCK) is considered as one of the major mediators that affect cell morphology [5], produces modifications in actin cytoskeletal apparatus [6], and regulates transcription factors leading to cellular hypertrophy [7].

Ferula assafoetida L. is a perennial herb of the *Umbelliferae* family that is widely distributed in Kashmir, Iran, Afghanistan, and India. The gum resin obtained by incision of the roots is known as a flavoring agent in food and a famous folklore medicine in Ayurveda, a traditional medicine native to India [8]. It is considered to a remedy for abdominal pain, constipation and diarrhea. Previous research has reported that gum resin extract of *F. assafoetida* exerts relaxation activities on intestinal smooth muscles and reducing blood pressure in anesthetized normotensive rats [9,10]. It

Abbreviations: Ang II, angiotensin II; ROCK, Rho-associated kinase; IMAP, immobilized metal affinity for phosphochemicals; TR-FRET, time-resolved fluorescence resonance energy transfer; MYPT, myosin phosphatase; MLC, myosin light chain; DMEM, Dulbecco's modified Eagle's medium.

* Corresponding author. Address: Research Center for Drug Discovery Technology, Korea Research Institute of Chemical Technology, 141 Gajeong-ro, Yuseong, Daejeon 305-343, Republic of Korea. Fax: +82 42 861 4246.
E-mail address: bhlee@krict.re.kr (B.H. Lee).

[1] These authors contributed equally to this work.

0006-291X/$ - see front matter © 2013 Elsevier Inc. All rights reserved.
http://dx.doi.org/10.1016/j.bbrc.2013.07.069

contains a variety of monosaccharides, ferulic acids and coumarin derivatives including sesquiterpene coumarins [11,12]. Kamolonol (7-[[(1*R*,2*R*,4*R*,4a*S*,5*R*,8a*S*)-4-hydroxy-1,2,4a,5-tetramethyl-6-oxo-3,4,5,7, 8,8a-hexahydro-2H-naphthalen-1-yl]methoxy]chromen-2-one; Fig. 1) is a sesquiterpene coumarin and an active component of *F. assafoetida*. Recently, we isolated kamolonol from the gum resin extract of *F. assafoetida*, and found that it possesses inhibitory activity against angiotensin II (Ang II)-induced stress fiber formation. To date, however, there is little information about the pharmacological actions of kamolonol in cardiovascular disease associated with fibrosis and cardiac hypertrophy. Therefore, the present study was performed to evaluate the anti-fibrotic as well as anti-cellular hypertrophic effects of kamolonol and further to explore the possible mechanism underlying these effects of kamolonol.

2. Materials and methods

2.1. Materials

Y27632 [4-(1-aminoethyl)-*N*-(4-pyridyl) cyclohexanecarboxamide dihydrochloride monohydrate], a specific inhibitor of ROCK [13], was purchased from Sigma–Aldrich (St. Louis, MO, USA). Human recombinant Rho-associated kinase 2 (ROCK2) was purchased from Upstate (Millipore Co, Billerica, MA, USA). The fluorescent peptide substrate (FAM-S6 ribosomal protein-derived peptide) and an immobilized metal affinity for phosphochemicals (IMAP)-based time-resolved fluorescence resonance energy transfer (TR-FRET) Screening Express Kit were obtained from MDS Analytical Technologies (Sunnyvale, CA, USA). 384-Well white flat-bottom plates were purchased from Corning Life Sciences (Lowell, MA, USA). Dulbecco's modified Eagle's medium (DMEM), fetal bovine serum, and antibiotics were purchased from GIBCO BRL (Grand Islang, NY, USA). Anti-myosin phosphatase 1 (MYPT1), anti-phosphorylated MYPT1 (anti-p-MYPT1), anti-myosin light chain 2 (anti-MLC2), and anti-phosphorylated MLC2 (anti-p-MLC2) rabbit polyclonal antibodies were purchased from Cell Signaling Technology (Danvers, MA, USA). Alexa fluor 586 phalloidin (F-actin probe) was purchased from Invitrogen (Carlsbad, CA, USA).

2.2. Isolation and identification of kamolonol

Commercially available Asafoetida (gum resin of *F. assafoetida*) was purchased from Arjuna Natural Extracts Ltd., Kerala, India. The voucher specimen (KR0176) was authenticated by Prof. Young-Kyoon Kim and deposited at the herbarium of the Korea Research Institute of Chemical Technology. The gum resin of *F. assafoetida* (1.2 kg) was extracted with methanol (20 L) three times at room temperature for 7 days. Concentration of the solvent gave 460 g of extract, which was suspended in water and then partitioned with *n*-hexane (56 g), dichloromethane (290 g), and *n*-butanol (50 g) successively. The dichloromethane layer (5 g) was suspended in 100 ml dichloromethane and subjected to chromatography on silica gel column (3.0 × 80 cm), eluted with dichloromethane–methanol by stepwise gradient (100:0 → 50:0 → 10:1), to yield four fractions. Among them, fraction 2 (570 mg) was purified by repeated silica gel column chromatography eluting with hexane/ethylacetate to afford 120 mg of kamolonol. Isolated kamolonol was identified by a direct comparison of physical and spectral properties (^{1}H NMR and ^{13}C NMR).

2.3. Cell culture

Rat heart-derived H9c2 cells were purchased from the American Type Culture Collection (ATCC, Rockville, MD, USA) and

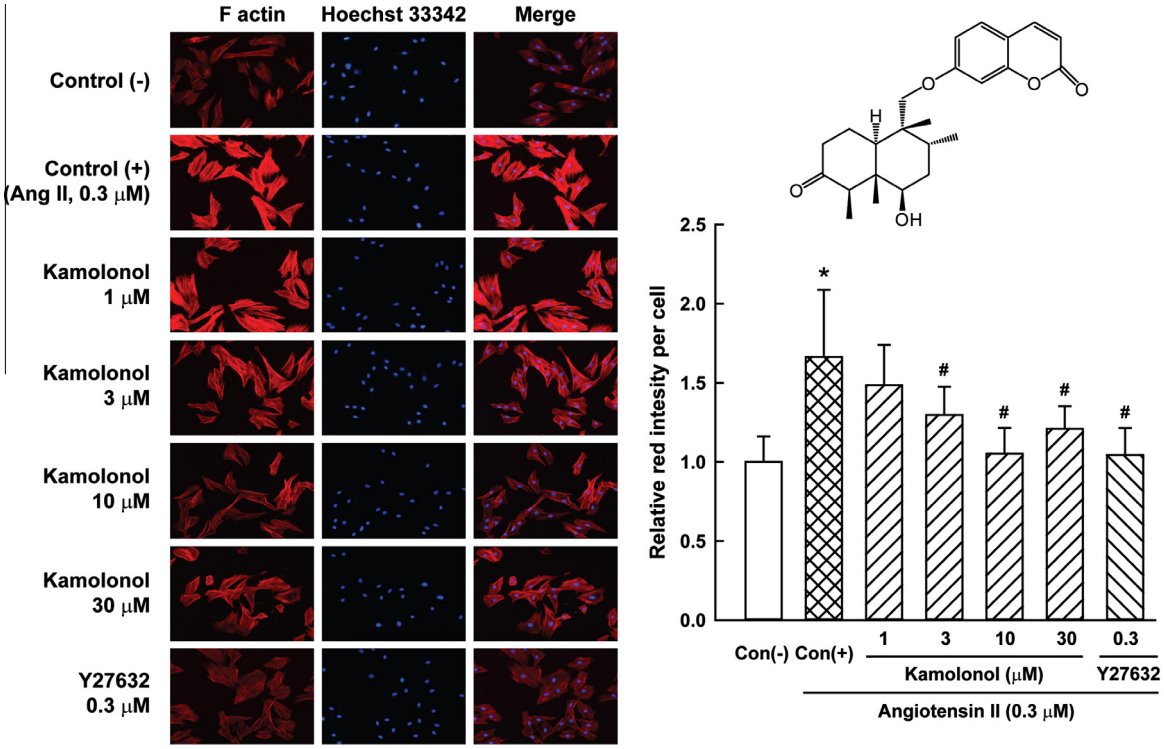

Fig. 1. Chemical structure of kamolonol and immunofluorescent staining for actin stress fiber formation in H9c2 cells. Cells were pretreated with kamolonol at the indicated concentrations for 2 h, and then stimulated with angiotensin II (Ang II, 0.3 μM) for 1 h. Actin stress fiber formation was visualized using an Alexa fluor 586 phalloidin. The same fields were counter stained with Hoechst 33342 dye for the location of the nuclei. Data are expressed as the mean ± S.D. (n = 7). $^*P < 0.05$, significantly different from control (−), $^\#P < 0.05$, significantly different from control (+) stimulated with Ang II (0.3 μM).

maintained at 1×10^6 cells/ml in DMEM supplemented with 10% fetal bovine serum, penicillin G (100 IU/ml), streptomycin (100 μg/ml), and L-glutamine (2 mM) in a 37 °C humidified atmosphere containing 5% CO_2 and 95% air. Cells were then starved in serum free media for 3 h and stimulated with 0.1 or 0.3 μM Ang II in the presence or absence of kamolonol (1–30 μM) at the indicated times. Stock solutions of kamolonol were prepared in dimethyl sulfoxide, and the maximum concentration of dimethyl sulfoxide in experimental media was 0.1%. Cells were cultured (37 °C, 5% CO_2) in a 16 well chamber slide (for immunofluorescent staining) or in 6 well plates (for western blotting or cellular hypertrophy). Cells were used at the following passage numbers: H9c2 cells (P_{3-15}).

2.4. Immunofluorescent staining for F-actin stress fiber formation

For immunofluorescent staining, H9c2 cells were plated on a chamber slide (Thermofisher, Rochester, NY, USA) at 1×10^5 cells/ml. After preincubation with or without kamolonol (1–30 μM) for 1 h, they were treated with Ang II (0.3 μM) for 2 h, fixed with 4% paraformaldehyde for 20 min, incubated with 0.5% Triton X-100 for 5 min at −20 °C in a freezer, and then blocked with 1% bovine serum albumin for 30 min. Cells were then probed with Alexa fluor 586 phalloidin (Invitrogen, Carlsbad, CA, USA, diluted 1:1000) for 30 min at room temperature in the dark, washed with phosphate-buffered saline solution three times, and stained with Hoechst 33342 dye for 2 min. Fluorescent images were obtained under a fluorescence microscope at 400× magnification (Nikon, Tokyo, Japan).

2.5. Cellular hypertrophy measurement

Cellular hypertrophy was measured from H9c2 cells treated with Ang II (0.3 μM) for 4 consecutive days as previously described [14]. For the study of cellular hypertrophy, cells were seeded at a density of 3×10^4 cells per 35-mm well of six-well plates and cultured for 24 h in DMEM containing 10% fetal bovine serum. Cells were washed with serum-free medium (DMEM without serum) and then treated with kamolonol (1–30 μM) under serum-free conditions for 24 h. Cells were treated with potential hypertrophic agonists, Ang II (0.3 μM) in quiescence medium (DMEM with 0.5% fetal bovine serum) with or without a fresh supply of kamolonol. Following this, cells were incubated for another 4 days at 37 °C in a humidified atmosphere containing 5% CO_2 to induce hypertrophic responses. After inducing cellular hypertrophy, adherent cells were fixed with 1% glutaraldehyde (Sigma–Aldrich) in phosphate buffered saline for 30 min and stained with 0.1% Crystal violet (Sigma–Aldrich) for 10 min. Images were obtained using a digital camera attached to an inverted microscope (Nikon) for analysis. Four random photographs were taken from each sample, and at least 140 individual cells were examined in each group. Cell size was analyzed using Image-Pro PLUS software (Media Cybernetics, Silver Spring, MD, USA). The data shown represent image analysis from three independent experiments.

2.6. Time-resolved fluorescence resonance energy transfer assay for ROCK2

ROCK2 assay was performed using 0.1 μg/ml ROCK2 in kinase reaction buffer (10 mM Tris–HCl, pH 7.2, 10 mM $MgCl_2$, 0.05%

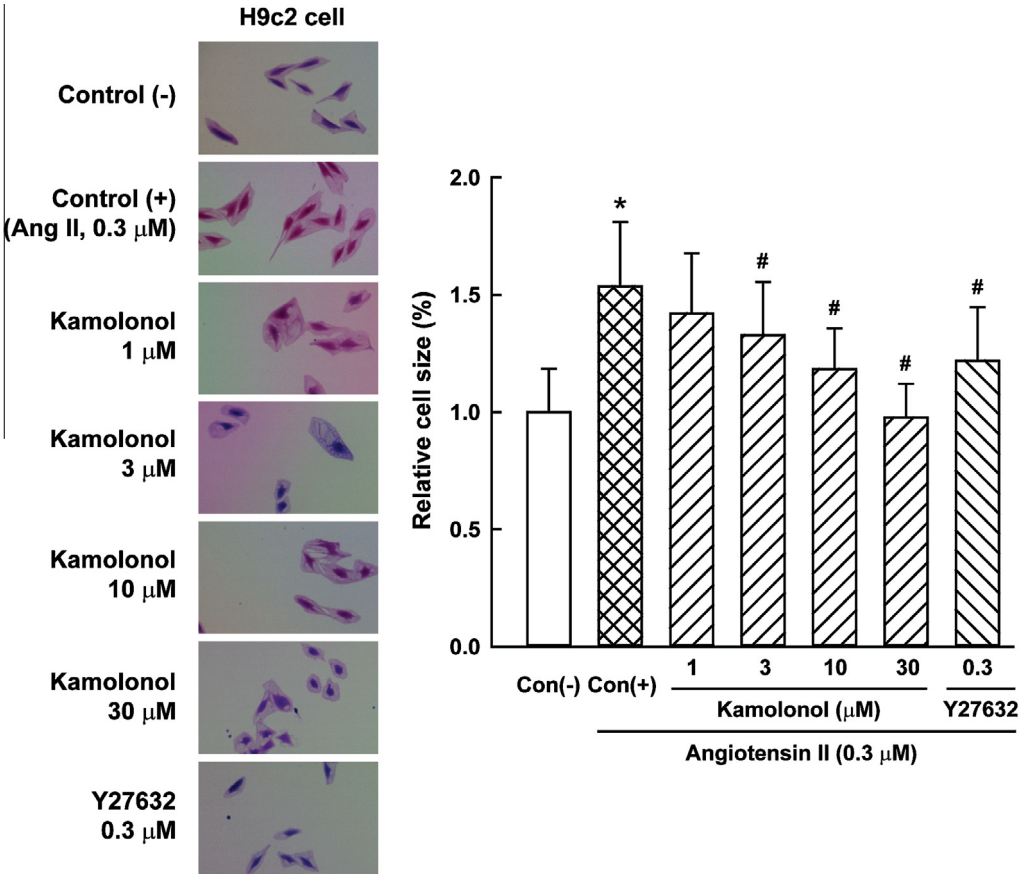

Fig. 2. Effects of kamolonol on cellular hypertrophy induced by angiotensin II (Ang II) in H9c2 cells. Cell size was analyzed using Image-Pro PLUS software, and the data are expressed as the relative mean area ± S.D. ($n = 21$). $^*P < 0.05$, significantly different from control (−), $^{\#}P < 0.05$, significantly different from control (+) stimulated with Ang II (0.3 μM).

NaN_3), containing 0.01%, Tween-20 and 1 mM dithiothreitol as previously reported [15]. Fluorescein-tagged S6 ribosomal protein-derived substrate (5FAM-AKRRRLSSLRA-COOH) and ATP were used with a final concentration of 1 or 3 μM, respectively. The total reaction volume was 20 μl and kamolonol (0.001–30 μM) was preincubated with ROCK2 for 10 min before adding the S6 ribosomal protein-derived substrate and ATP. Kinase reactions were conducted for 45 min at room temperature in white standard 384-well plates and then 60 μl of detection mixture (1:600 dilution of IMAP binding reagent and 1:400 dilution of Terbium donor supplied by MDS Analytical Technologies) was added to kinase reaction plates 3 h before reading the plates. The TR-FRET counts were measured using the Envision (PerkinElmer Oy, Turku, Finland) multilabel counter with a TR-FRET option. The instrument settings used were 340 nm for excitation and 520 nm and 495 nm for emission with a 100 μs delay time. Measured TR-FRET counts were used to calculate percent inhibitions and IC_{50} values.

2.7. Immunoblot for myosin phosphatase 1 and myosin light chain 2

H9c2 cells were treated with or without kamolonol (1–30 μM) for 2 h before Ang II stimulation. Cells were then stimulated with 0.1 μM Ang II for 15 min to determine levels of myosin phosphatase 1 (MYPT1), myosin light chain 2 (MLC2), phosphorylated MYPT1 (p-MYPT1), and phosphorylated MLC2 (p-MLC2). Ang II-stimulation was stopped by adding ice-cold phosphate-buffered saline. The cells were then lysed for immunoblotting. Equal amounts of extracted proteins were separated on 12% or 6% SDS–polyacrylamide gels, transferred to nitrocellulose membranes. Blots were probed with rabbit polyclonal antibodies against MYPT1, p-MYPT1, MLC2, and p-MLC2. Proteins transferred to membranes were detected using the LumiGLO kit (New England Biolabs, Ipswich, MA, USA). All antibodies were purchased from Cell Signaling (Danvers, MA, USA) and used at a dilution of 1:1000.

2.8. Statistical analysis

All values are expressed as means ± SDs. Data were analyzed by one-way analysis of variance (ANOVA), followed by Dunnett's test for multiple comparisons (Sigma Stat, Jandel Co., San Rafael, CA, USA). Concentration-response curves were analyzed by nonlinear regression using PRISM version 3.0 (GraphPad Software Inc., La Jolla, CA, USA), and the IC_{50} value of kamolonol (the concentration required to reduce the TR-FRET count to 50% of the positive control) was calculated. In all comparisons, statistical significance was accepted for P values of <0.05.

3. Results

3.1. Cellular effects of kamolonol on actin stress fiber formation

To evaluate the cellular effect of kamolonol, we used an actin stress fiber formation assay. As shown in Fig. 1, treatment with Ang II (0.3 μM) alone (Control (+)) for 2 h caused an increase of actin stress fiber formation by approximately 1.7 times. This increase of actin stress fiber formation induced by Ang II was significantly suppressed by pretreatment with kamolonol (3–30 μM). This suppressive effect on actin stress fiber formation was also observed with 0.3 μM Y27632, a specific ROCK inhibitor.

3.2. Effects of kamolonol on cellular hypertrophy induced by Ang II in H9c2 cells

In control H9c2 cells treated with Ang II (0.3 μM) alone (Control (+)) for 4 consecutive days, cell size was significantly increased by approximately 1.5 times (Fig. 2). The increase in cell size induced by Ang II was inhibited by pretreatment with kamolonol in a concentration-dependent manner. In particular, cellular hypertrophy induced by Ang II was significantly inhibited by concentrations above 3 μM of kamolonol and completely blocked by 30 μM. Such inhibitory effect on cellular hypertrophy was also observed with 0.3 μM Y27632.

3.3. Inhibitory effects of kamolonol on ROCK2

The inhibitory effects of kamolonol on the activities of ROCK2 were evaluated using a kinase assay based on IMAP-TR-FRET, which involves specific interactions between proprietary nanoparticles and covalent phosphorylated moieties. Phosphosubstrate–nanoparticle binding events can be directly quantified and expressed as TR-FRET counts, which reflect the amount of ROCK-induced phosphorylation of a substrate. The assay conditions of ROCK2-IMAP-TR-FRET assays were verified using Y27632 as a reference compound (IC_{50} values: 0.23 μM), which agreed with the

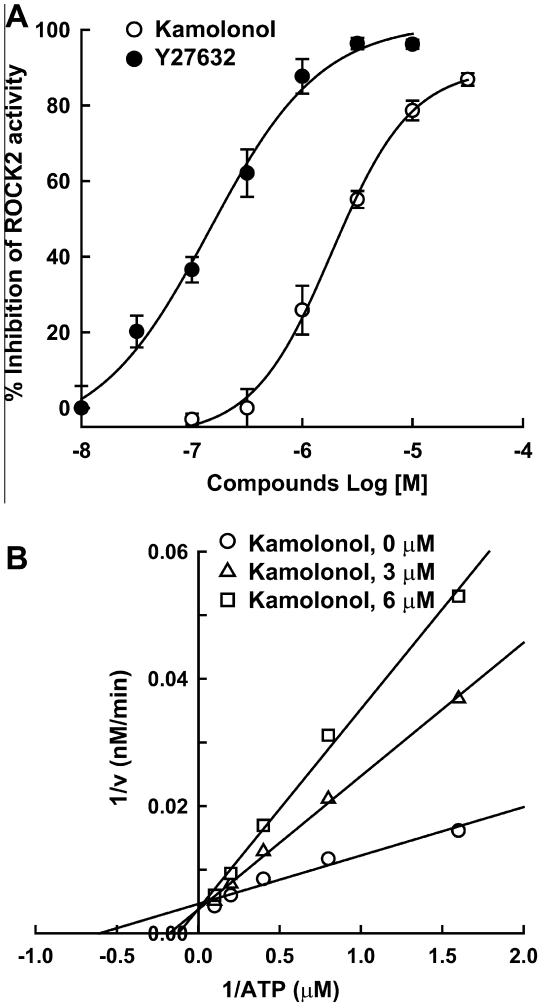

Fig. 3. Inhibitory effect of kamolonol on Rho-associated kinase 2 (ROCK2) activity (A), and inhibitory mode of kamolonol (B). The ROCK2 activity was determined by IMAP-TR-FRET as described in the Materials and Methods sections. Y27632 was used as a reference compound for ROCK2 assay. The percent inhibition was calculated as ([raw data of compound–$Mean_{c-}$]/[$Mean_{c+}$–$Mean_{c-}$]) × 100. Data are expressed as the mean ± S.D. (n = 3). Double reciprocal plots of 1/v versus 1/[ATP] were carried out using varying concentrations of ATP (0.625–10 μM), ROCK2 (0.1 μg/multilabel), and substrate (1 μM) in the presence or absence of kamolonol. The initial rate v was estimated as an amount of phospho-substrate transferred during the reaction period (nM/min).

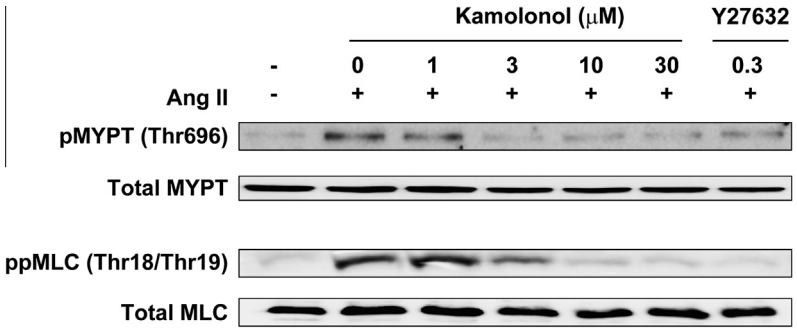

Fig. 4. Inhibitory effects of kamolonol against angiotensin II (Ang II)-induced phosphorylation of myosin phosphatase 1 (MYPT1) and myosin light chain 2 (MLC2). Cells were pre-incubated for 2 h with or without kamolonol at the indicated concentrations and then stimulated with Ang II (0.1 μM). Detection of the total MYPT1 and MLC2 was estimated by protein-loading control for each lane.

IC_{50} values obtained using a radio-isotope based kinase assay (0.3 μM) [13]. As shown in Fig. 3A, kamolonol inhibited the ROCK2-induced TR-FRET counts in a concentration-dependent manner, and provided IC_{50} values of 2.27 μM.

In the inhibition mode studies, double reciprocal plots of $1/v$ versus 1/[ATP] were performed using various concentrations of ATP (0.625–10 μM), ROCK2 (0.1 μg/ml), and S6 ribosomal protein-derived substrate (1 μM) in the presence or absence of kamolonol. The initial rate v was defined as rate of phospho-substrate transfer (nM/min). As shown in Fig. 3B, kamolonol behaved as an ATP-competitive inhibitor of ROCK2.

3.4. Inhibitory effects of kamolonol on MYPT1 and MLC2 phosphorylation in activated H9c2 cells

To assess the effects of kamolonol on the phosphorylations of MYPT and MLC via ROCK activation, we prepared extracts of H9c2 cells activated with Ang II and determined phosphorylated MYPT1 and MLC2 levels by immunoblotting. As shown in Fig. 4, treatment with 0.1 μM Ang II for 15 min caused the phosphorylations of MYPT1 and MLC2 in H9c2 cells and these Ang II-induced phosphorylations were decreased by pretreatment with kamolonol (3–30 μM). In the same experiment, the phosphorylation of MYPT1 and MLC2 were inhibited by pretreatment with Y27632 (0.3 μM).

4. Discussion

Recently, we isolated kamolonol from the gum resin extract of *F. assafoetida*. Kamolonol (7-[[(1*R*,2*R*,4*R*,4a*S*,5*R*,8a*S*)-4-hydroxy-1,2,4a,5-tetramethyl-6-oxo-3,4,5,7, 8,8a-hexahydro-2H-naphthalen-1-yl]methoxy]chromen-2-one) is comprised in a sesquiterpene with coumarin residue. To date, there is little information about the pharmacological actions of kamolonol besides to antiplasmodial activity [16]. In the present study, we found that kamolonol markedly inhibited Ang II-induced actin stress fiber formation in H9c2 cells. On increasing the concentration of kamolonol, thin central stress fibers were gradually lost, whereas thick peripheral stress fibers remained. These results are typical of ROCK inhibition [17], and it is well known that ROCK plays a pivotal role in the organization of actin filaments in cells including formation of stress fibers [6,18]. Furthermore, kamolonol significantly and concentration-dependently suppressed the increase in cell size induced by Ang II in the cellular hypertrophy study. Cellular hypertrophy is associated with distinct morphological changes in cell shape and remodeling of the actin cytoskeleton. ROCK appears to be an important mediator to affect cell morphology [5,19], through regulation of actin cytoskeletal apparatus [6] and cellular hypertrophic gene expression [7,20]. Based on these considerations, we hypothesized that the anti-fibrotic and anti-cellular hypertrophic effect of kamolonol may be due to blocking the ROCK-signaling pathway.

Although there are both isoforms of ROCK1 and ROCK2, ROCK2 activity was measured because ROCK2 is mostly expressed in heart and brain [21,22]. As we expected, ROCK2-TR-FRET assay revealed that kamolonol possesses a potent ability to inhibit ROCK2 with IC_{50} values of 2.27 μM and behaves as an ATP-competitive inhibitor. The ROCK2-TR-FRET assay was standardized for the optimum concentration of the individual components of ROCK2, substrate, ATP, Tb-donor, and nanoparticle [15]. In addition, this assay was validated with Y27632 a standard inhibitor, prior to screening of kamolonol. These results suggest that kamolonol potently inhibits ROCK2 and that by so doing it modulates actin stress fiber formation and cellular hypertrophy. These anti-fibrotic and anti-cellular hypertrophic effects of kamolonol explain, at least in part, its pharmacology and mode of action.

Phosphorylation of MYPT by ROCK inhibits phosphatase activity [23], leading to increased MLC phosphorylation and subsequent enhancement of stress fiber formation [1]. To confirm ROCK2 inhibitory activity of kamolonol, we investigated whether kamolonol regulates the phosphorylations of MYPT and MLC. In the present study, immunoblot analysis showed that the kamolonol decreased the Ang II-induced phosphorylations of MYPT1 and MLC2. Of the multiple substrates involved in ROCK signaling, MYPT is known to be a major downstream target [24]. MYPT regulates the interaction of actin and myosin in response to signaling through ROCK activation. The phosphorylation of MYPT1 at Thr696 by ROCK results in phosphatase inhibition and cytoskeletal reorganization [25]. ROCK also regulates the activity of MLC by direct MLC phosphorylation [26]. ROCK phosphorylates Ser19 of MLC2, which directly regulates the assembly of actin stress fiber [27].

In conclusion, our results showed for the first time that kamolonol suppresses the stress fiber formation and cellular hypertrophy in Ang II-stimulated H9c2 cells. In addition, the results in the present study suggest that kamolonol possesses a potent ROCK2 inhibitory activity, and that ROCK2 inhibition suppresses actin stress fiber formation and cellular hypertrophy by inhibiting the phosphorylations of MYPT and MLC. However, further studies are necessary to elucidate the molecular entities directly responsible.

Acknowledgments

This study was supported by a Grant of the Bio & Medical Technology Development Program (2011-0019397) of the National Research Foundation (MRF) funded by MEST, and by a Grant of the Technology Innovation Program (10038744) of Korea Evaluation Institute of Industrial Technology (KEIT) funded by MKE, Republic of Korea.

Appendix A. Supplementary data

Supplementary data associated with this article (^{1}H NMR and ^{13}C NMR spectral data of kamolonol) can be found, in the online version, at http://dx.doi.org/10.1016/j.bbrc.2013.07.069.

References

[1] S. Pellegrin, H. Mellor, Actin stress fibres, J. Cell Sci. 120 (2007) 3491–3499.
[2] C. Chaponnier, G. Gabbiani, Pathological situations characterized by altered actin isoform expression, J. Pathol. 204 (2004) 386–395.
[3] L. Jin, The actin associated protein palladin in smooth muscle and in the development of diseases of the cardiovasculature and in cancer, J. Muscle Res. Cell Motil. 32 (2011) 7–17.
[4] C.M. Yu, G.L. Tipoe, K. Wing-Hon Lai, C.P. Lau, Effects of combination of angiotensin-converting enzyme inhibitor and angiotensin receptor antagonist on inflammatory cellular infiltration and myocardial interstitial fibrosis after acute myocardial infarction, J. Am. Coll. Cardiol. 38 (2001) 1207–1215.
[5] A. Lai, W.H. Frishman, Rho-kinase inhibition in the therapy of cardiovascular disease, Cardiol. Rev. 13 (2005) 285–292.
[6] A.J. Ridley, A. Hall, The small GTP-binding protein rho regulates the assembly of focal adhesions and actin stress fibers in response to growth factors, Cell 70 (1992) 389–399.
[7] K. Kuwahara, T. Barrientos, G.C. Pipes, S. Li, E.N. Olson, Muscle-specific signaling mechanism that links actin dynamics to serum response factor, Mol. Cell. Biol. 25 (2005) 3173–3181.
[8] L. Boulus, Medicinal Plants of North Africa, NHBS Environment Bookstore, Algonae, 1983. 183.
[9] M. Fatehi, F. Farifteh, Z. Fatehi-Hassanabad, Antispasmodic and hypotensive effects of *Ferula assafoetida* gum extract, J. Ethnopharmacol. 91 (2004) 321–324.
[10] P. Mahendra, S. Bisht, *Ferula assafoetida*: traditional uses and pharmacological activity, Pharmacogn. Rev. 6 (2012) 141–146.
[11] M.H. Abd El-Razek, S. Ohta, A.A. Ahmed, T. Hirata, Sesquiterpene coumarins from the roots of *Ferula assafoetida*, Phytochemistry 58 (2001) 1289–1295.
[12] M.R. Cha, Y.H. Choi, C.W. Choi, Y.S. Kim, Y.K. Kim, S.Y. Ryu, Y.H. Kim, S.U. Choi, Galbanic acid, a cytotoxic sesquiterpene from the gum resin of *Ferula assafoetida*, blocks protein farnesyltransferase, Planta Med. 77 (2011) 52–54.
[13] T. Ishizaki, M. Uehata, I. Tamechika, J. Keel, K. Nonomura, M. Maekawa, S. Narumiya, Pharmacological properties of Y-27632, a specific inhibitor of rho-associated kinases, Mol. Pharmacol. 57 (2000) 976–983.
[14] G.S. Hwang, K.S. Oh, H.N. Koo, H.W. Seo, K.H. You, B.H. Lee, Effects of KR-31378, a novel ATP-sensitive potassium channel activator, on hypertrophy of H9c2 cells and on cardiac dysfunction in rats with congestive heart failure, Eur. J. Pharmacol. 540 (2006) 131–138.
[15] K.S. Oh, J. Mun, J.E. Cho, S. Lee, K.Y. Yi, C.J. Lim, J.S. Lee, W.J. Park, B.H. Lee, Discovery of novel scaffolds for Rho kinase 2 inhibitor through TRFRET-based high throughput screening assay, Comb. Chem. High Throughput Screen. 16 (2013) 37–46.
[16] D. Dastan, P. Salehi, A. Reza Gohari, S. Zimmermann, M. Kaiser, M. Hamburger, H. Reza Khavasi, S.N. Ebrahimi, Disesquiterpene and sesquiterpene coumarins from *Ferula pseudalliacea*, and determination of their absolute configurations, Phytochemistry 78 (2012) 170–178.
[17] K. Katoh, Y. Kano, M. Amano, K. Kaibuchi, K. Fujiwara, Stress fiber organization regulated by MLCK and Rho-kinase in cultured human fibroblasts, Am. J. Physiol. Cell Physiol. 280 (2001) C1669–C1679.
[18] M. Amano, K. Chihara, K. Kimura, Y. Fukata, N. Nakamura, Y. Matsuura, K. Kaibuchi, Formation of actin stress fibers and focal adhesions enhanced by Rho-kinase, Science 275 (1997) 1308–1311.
[19] A. Zeidan, S. Javadov, M. Karmazyn, Essential role of Rho/ROCK-dependent processes and actin dynamics in mediating leptin-induced hypertrophy in rat neonatal ventricular myocytes, Cardiovasc. Res. 72 (2006) 101–111.
[20] J.H. Brown, D.P. Del Re, M.A. Sussman, The Rac and Rho hall of fame: a decade of hypertrophic signaling hits, Circ. Res. 98 (2006) 730–742.
[21] O. Nakagawa, K. Fujisawa, T. Ishizaki, Y. Saito, K. Nakao, S. Narumiya, ROCK-I and ROCK-II, two isoforms of Rho-associated coiled-coil forming protein serine/threonine kinase in mice, FEBS Lett. 392 (1996) 189–193.
[22] H. Shimokawa, M. Rashid, Development of Rho-kinase inhibitors for cardiovascular medicine, Trends Pharmacol. Sci. 28 (2007) 296–302.
[23] K. Kimura, M. Ito, M. Amano, K. Chihara, Y. Fukata, M. Nakafuku, B. Yamamori, J. Feng, T. Nakano, K. Okawa, A. Iwamatsu, K. Kaibuchi, Regulation of myosin phosphatase by Rho and Rho-associated kinase (Rho-kinase), Science 273 (1996) 245–248.
[24] M. Terrak, F. Kerff, K. Langsetmo, T. Tao, R. Dominguez, Structural basis of protein phosphatase 1 regulation, Nature 429 (2004) 780–784.
[25] A.A. Birukova, K. Smurova, K.G. Birukov, P. Usatyuk, F. Liu, K. Kaibuchi, A. Ricks-Cord, V. Natarajan, I. Alieva, J.G. Garcia, A.D. Verin, Microtubule disassembly induces cytoskeletal remodeling and lung vascular barrier dysfunction: role of Rho-dependent mechanisms, J. Cell. Physiol. 201 (2004) 55–70.
[26] Y. Kawano, Y. Fukata, N. Oshiro, M. Amano, T. Nakamura, M. Ito, F. Matsumura, M. Inagaki, K. Kaibuchi, Phosphorylation of myosin-binding subunit (MBS) of myosin phosphatase by Rho-kinase *in vivo*, J. Cell Biol. 147 (1999) 1023–1038.
[27] G. Totsukawa, Y. Yamakita, S. Yamashiro, D.J. Hartshorne, Y. Sasaki, F. Matsumura, Distinct roles of ROCK (Rho-kinase) and MLCK in spatial regulation of MLC phosphorylation for assembly of stress fibers and focal adhesions in 3T3 fibroblasts, J. Cell Biol. 150 (2000) 797–806.